

**Final Report
Earthquake Hazards Program Assistance Awards**

USGS Award Number(s)

G13AP00053

Title of award

Inter-seismic Locking on the Cascadia Subduction Zone

Author(s)

Robert McCaffrey
Portland State University
Dept. of Geology
Portland OR 97207-0751
phone: 518.369.5268
fax: 503.725.3025
r.mccaffrey@pdx.edu

Term covered by the report: July 1, 2013 – August 30, 2014

Abstract: GPS observations were made along the Oregon coast and coast ranges, Oregon, in 2013 and 2014 with the goal of resolving in more detail the distribution of locking on the Cascadia subduction zone (CSZ). The new GPS velocities were used along with leveling data in models to estimate the locking patterns on the CSZ and to compare to predicted locking patterns based on other CSZ properties. The results indicate that locking models based on thermal predictions do not produce the correct along-strike variations. The basin (gravity lows) model of Wells et al. (2003) also does not in detail predict where the CSZ is currently being loaded. The current data can resolve along-strike variations in locking at the scale of about 40 km. That scale of variation is required to match the latest available geodetic data.

Report:

Introduction

The Cascadia subduction zone has the potential of producing one of the country's greatest natural disasters. Mitigating that disaster is among the more important tasks assigned to our nation's hazards research. One critical step is to map the spatial variability in slip potential along the entire plate interface. Some work has suggested that the slip in the 2011 Tohoku-oki earthquake mimicked in a broad sense the pre-quake locking distribution. At the present time, geodetic data offer our best constraints on the locking distribution on the Cascadia subduction zone. The work done here is to use geodetic data in the forms of the three components of GPS velocities, leveling-based uplift rates and tide-gauge uplift rates to understand the range of locking distributions that may be allowable by the data. In addition to modeling based on the existing horizontal and vertical geodetic data, we collected GPS measurements at 28 coastal sites in Oregon to help constrain rates there. The locking distributions can be used to make estimates of the slip distribution during a great earthquake for ground motion models and also to predict seafloor vertical motions that are used in tsunami simulations. The modeling effort also provides estimates of slip rates and frictional locking on crustal faults in Oregon and Washington.

Investigations undertaken

We conducted GPS field work in September 2013 and August 2014 to occupy geodetic benchmarks within and around coastal Oregon. Our target sites were those survey-mode sites that had not been occupied within the past 10 years with the aim of obtaining velocities with uncertainties as low as 0.3 mm/yr. The scientific goal is to understand the distribution of locking on the Cascadia subduction zone and its implications for earthquake hazards in the Pacific Northwest (PNW).

2013 Field season. We borrowed (at no cost) five high-precision field GPS units from the UNAVCO pool for six weeks from early September to mid October, 2012. The UNAVCO engineers were very helpful in fixing some small problems with the receivers. McCaffrey and Central Washington University undergrad Wade Holter were in the field 7 days and occupied 15 sites along the coast from Northernmost California to Lincoln City. Sites north of Lincoln City had been done recently by us (McCaffrey et al., 2013), in 2011 so were not repeated.

2014 Field season. The field work in 2014 followed the same procedure as in 2013. We were able to re-occupy 13 sites that showed spurious results after modeling our 2013 measurements. In particular sites within the Willamette Valley and the eastern Coast Ranges between Corvallis and Eugene OR showed systematic easterly residuals. This region is part of the Newport section of the subduction zone that shows anomalously low uplift rates and the new data help resolve why.

Data Processing. We are now finishing up processing the field data we collected along with data from continuous GPS sites in the region (the PANGA and PBO networks). We acquired survey-mode data from USGS sites in the area that were measured by Wayne Thatcher, Mike Lisowski and colleagues. The processing is being done by Robert W. King at MIT (at no cost to this grant) using GAMIT and GLOBK (Herring et al., 2010) largely in the manner described in McCaffrey et al. (2007).

Results. Fig. 1 shows the sites we occupied in 2013 and 2014 along with the regional continuous networks (PBO and PANGA). We were able to re-occupy most of the targeted survey-mode sites (purple dots). Figs. 2 and 3 show estimates of the site velocities calculated in September, 2014, relative to North America. The data include the PBO and PANGA observation as well as our own survey observations processed together. The new velocities are much more systematic and have greatly reduced uncertainties relative to the previous field. The large-scale rotation of Oregon and adjacent regions is well-established by the new velocity field. This rotation is long-lived; evident in paleomag results from the Columbia River Basalts and in offsets of the Cascade arc volcanoes (Wells and McCaffrey, 2012). Removal of the rotational component along the coast reveals the substantial velocities due largely to locking at Cascadia (Fig. 4).

We have run several models to estimate locking on the Cascadia thrust. The block model that forms the basis of the crustal deformation is shown in Fig. 5. It is similar to those presented earlier by us (McCaffrey et al., 2007; 2013; Payne et al 2008; 2012) with changes largely in the Yakima fold-thrust belt and along the Cascade arc. The shape of the Cascadia plate interface is taken from McCrory et al. (2012) sampled along strike and downdip to use with the modeling program TDEFNODE (McCaffrey, 2009).

The modeling uses the new GPS velocity field along with leveling data from Oregon (Burgette et al., 2009) and more recent leveling from Washington (obtained from Reed Burgette, 9/30/14). The locking models attempt to fit all the data (1926 observations) simultaneously and the fits are given in Table 1. While we generated a greater number of models, only a few are described here.

The models PN00, PN01 and PN08 use three different parameterizations of the locking distribution that all allow both along-strike and down-dip variations. PN00 (Fig. 6) assumes that the locking follows a Gaussian distribution with depth but allows arbitrary variation along-strike, subject to Laplacian smoothing (see McCaffrey et al., 2013). PN01 (Fig. 7) uses a grid distribution to the locking pattern where patches are assumed to have uniform locking but the locking can vary from patch to patch, with Laplacian smoothing along-strike and down-dip. For PN08 (Fig. 8) we use an exponential function to describe the locking with depth, as suggested by Wang et al. (2003) and implemented by McCaffrey et al. (2007), again with along-strike Laplacian smoothing.

The fits to the data (Table 1) indicate that the grid model (Fig. 7) is best followed by the Gaussian (Fig. 6) and then the exponential model (Fig. 8). The maps in each figure show the GPS velocity residuals indicating where the misfits are prominent. Large residuals occur in the south of Oregon and northern California where the slab structure and surface tectonics are both complex. The grid model does best there by allowing some deeper locking on the subduction fault. The exponential model (Fig. 8) also has difficulty matching velocities about 100 km inland of the coast in central Oregon. In Washington, the models seem to fit the data equally well. The dominant feature is high locking off the Olympic Peninsula.

In other models, we tested whether locking could be uniform along strike with the exponential model (PN07; Fig. 9), or if it is localized beneath forearc basins (PN11; Fig. 10) as suggested by Wells et al. (2003). In PN14 (Fig. 11) we tested the Fluck et al. (2007) slab structure and locking based on the Hyndman and Wang (1993; 1995) thermal models that allowed variation along strike. These three models did a very poor job of fitting the modern geodetic data (Table 1) with reduced chi-squared values of 10 or more.

In Fig. 12 we compare the models PN00 (Gaussian), PN01 (grid) and PN11 (forearc basins) to vertical data along the Columbia River transect at 46.25N (Burgette et al., 2009). The Gaussian and grid models do a good job of matching the observations while the Wells et al. (2003) basin model underestimates the uplift rates.

We performed a checkerboard test of the resolution for locking (Fig. 13). A presumed distribution of locking (Fig. 13a) was used to generate velocities and uplift rates at the observation points. To these velocities were added random errors that followed the distributions of the real data uncertainties. Then the data were used to solve for the locking on the subduction zone using a grid model. To test for dependence on the starting model, in the first run (Fig. 13b) the starting model comprised a completely locked fault and in the second run (Fig. 13c) the starting model was completely free-slip (zero locking everywhere). The results of the two inversions are very similar. They indicate that offshore (depths less than 15 km) the locking is not recovered very well and the data lack resolution. Closer to shore and where the plate interface is deeper than 15 km, the data faithfully recover the test model. The patches in the recovery test are spaced at about 40 km and these are recovered, indicating this level of spatial resolution.

Problems encountered

Mark Y726 near Eddyville OR was located but is now beneath a large bush. The caretaker indicated the bush could be cut down but we did not occupy the mark. Mark G728, southeast of Corvallis, was destroyed by a farmer plowing the field. We found the bent stainless-steel rod still in place but the mark could not be occupied. The marks we call PETE (Peterson Butte) and TWN3 (Indian Head) were not accessible due to fire hazard concerns by the landowners. On the other hand, we recovered mark EDDY in 2014, near Eddyville, that we thought was lost in 2013.

We hiked to the mark (MRY5) atop Mary's Peak, but otherwise all others were close to roads. More information about the marks we visited is available on the log sheets archived at UNAVCO.

Data availability

GPS field data (raw and rinex form) and logsheets collected for this project are archived at UNAVCO (see Bibliography for data DOI). Final velocities will be included in publications.

Acknowledgments

Thanks to many landowners who gave us access to sites. To Wade Holder and John Omer who assisted in the field. Bob King processed the GPS data. Reed Burgette, Ray Weldon and David Schmidt provided new unpublished uplift data from Washington. Ray Wells assisted in developing the block models. GPS equipment and advice was provided at no cost from UNAVCO.

Table 1. Model statistics

Model	Reduced Chi**2	GPS Nrms	Vertical Nrms	Npar	Notes
PN00	3.96	2.07	1.38	208	Gaussian
PN01	3.05	1.80	0.85	380	Grid
PN07	10.78	2.89	3.70	124	Exp. Uniform
PN08	4.54	2.29	1.20	208	Exp. Variable
PN11	9.99	2.87	3.42	126	Wells basins
PN14	14.75	3.22	3.58	104	Fluck slab, H&W locking

Npar is number of free parameters. Exp. represents the exponential locking function of Wang et al. (2003). H&W indicates locking based on Hyndman and Wang (1993; 1995) thermal models.

Bibliography

- Burgette, R. J., R. J. Weldon, and D. A. Schmidt, (2009), Interseismic uplift rates for western Oregon and along-strike variation in locking on the Cascadia subduction zone: *J. Geophys. Res.*, 114, B01408, doi:10.1029/2008JB005679.
- Fluck, P., R. D. Hyndman, and K. Wang, (1997), Three-dimensional dislocation model for great earthquakes of the Cascadia subduction zone, *Jour. Geophys. Res.*, 102, 20,539-20,550.
- Herring, T.A., R. W. King and S. C. McCluskey., (2010). *Introduction to GAMIT/GLOBK, Release 10.4*, Massachusetts Institute of Technology, 48 p (<http://www-gpsg.mit.edu/~simon/gtgc/docs.htm>).
- Hyndman, R. D., and K. Wang, (1993). Thermal constraints on the zone of major thrust earthquake failure: The Cascadia subduction zone, *J. Geophys. Res.*, 98, 2039-2060.
- Hyndman, R. D., and K. Wang, (1995). The rupture zone of Cascadia great earthquakes from current deformation and the thermal regime, *J. Geophys. Res.*, 100, 22133-22154.
- McCaffrey, R., (2009), Time-dependent inversion of three-component continuous GPS for steady and transient sources in northern Cascadia: *Geophys. Res. Letts.*, 36, L07304, doi:10.1029/2008GL036784.
- McCaffrey, R., (2014), Cascadia 2014, UNAVCO, GPS Data Set, [doi:10.7283/T5D21VV5](https://doi.org/10.7283/T5D21VV5)
- McCaffrey, R., A. I. Qamar, R. W. King, R. Wells, G. Khazaradze, C. A. Williams, C. W. Stevens, J. J. Vollick, and P. C. Zwick, (2007). Fault locking, Block Rotation and Crustal Deformation in the Pacific Northwest, *Geophysical Journal International*, v. 169, p. 1315-1340, doi:10.1111/j.1365-246X.2007.03371.x.
- McCaffrey, R., Lancaster, M., (2012). Oregon 2011, UNAVCO, GPS Data Set, [doi:10.7283/T5B27SB8](https://doi.org/10.7283/T5B27SB8)
- McCaffrey, R., King, R. W., (2013). Yakima Fold Thrust Belt 2012, UNAVCO, GPS Data Set, [doi:10.7283/T56971NC](https://doi.org/10.7283/T56971NC)
- McCaffrey, R., R. W. King, S. J. Payne, and M. Lancaster, (2013). Active Tectonics of Northwestern US inferred from GPS-derived Surface Velocities, *J. Geophys. Res.*, 118, doi:10.1029/2012JB009473.
- McCaffrey, R., King, R. W., (2014). Yakima Fold Thrust Belt 2013, UNAVCO, GPS Data Set, doi:10.7283/T52J68Z3
- McCaffrey, R., R. W. King, and G. Schmalzle, (2014). Geodetic constraints on Cascadia locking, *Geological Society of America Abstracts with Programs*. Vol. 46, No. 6, p.443, paper 178-3.
- McCrory, P. A., J. L. Blair, F. Waldhauser, and D. H. Oppenheimer (2012). Juan de Fuca slab geometry and its relation to Wadati-Benioff zone seismicity, *J. Geophys. Res.*, 117, B09306, doi:10.1029/2012JB009407.
- Payne, S. J., R. McCaffrey, and R.W. King (2008), Strain rates and contemporary deformation in the Snake River Plain and surrounding Basin and Range from GPS and seismicity, *Geology*, 36, 647-650.
- Payne, S. J., R. McCaffrey, R.W. King and S.A. Kattenhorn (2012), A new interpretation of deformation rates in the Snake River Plain and adjacent Basin and Range regions based on GPS measurements, *Geophys. J. Inter.*, 189, 101-122, doi: 10.1111/j.1365-246X.2012.05370.x.
- Payne, S. J., R. W. King and R. McCaffrey, (2015). Update of GPS deformation rates in the Snake River Plain, in Lund, W.R., editor, Proceedings volume, Basin and Range Province Seismic-Hazards Summit III: Utah Geological Survey Miscellaneous

Publication.

- Schmalzle, G. M., R. McCaffrey, and K. Creager, (2014). Central Cascadia subduction zone creep, *Geophysics, Geochemistry, Geosystems*, doi: 10.1002/2013GC005172.
- Schmalzle, G., R. McCaffrey, and K. C. Creager, (2014). Cascadia subduction zone locking, Geological Society of America *Abstracts with Programs*. Vol. 46, No. 6, p.443, paper 178-4.
- Wang, K., R. Wells, S. Mazzotti, R. D. Hyndman and T. Sagiya (2003), A revised dislocation model of interseismic deformation of the Cascadia subduction zone, *J. Geophys. Res.*, 108, 2026, doi:10.1029/2001JB001227.
- Wells, R., and R. McCaffrey, (2013). Rotation of the Cascade Arc, *Geology*, 41, 1027-1030, doi: 10.1130/G34514.1.

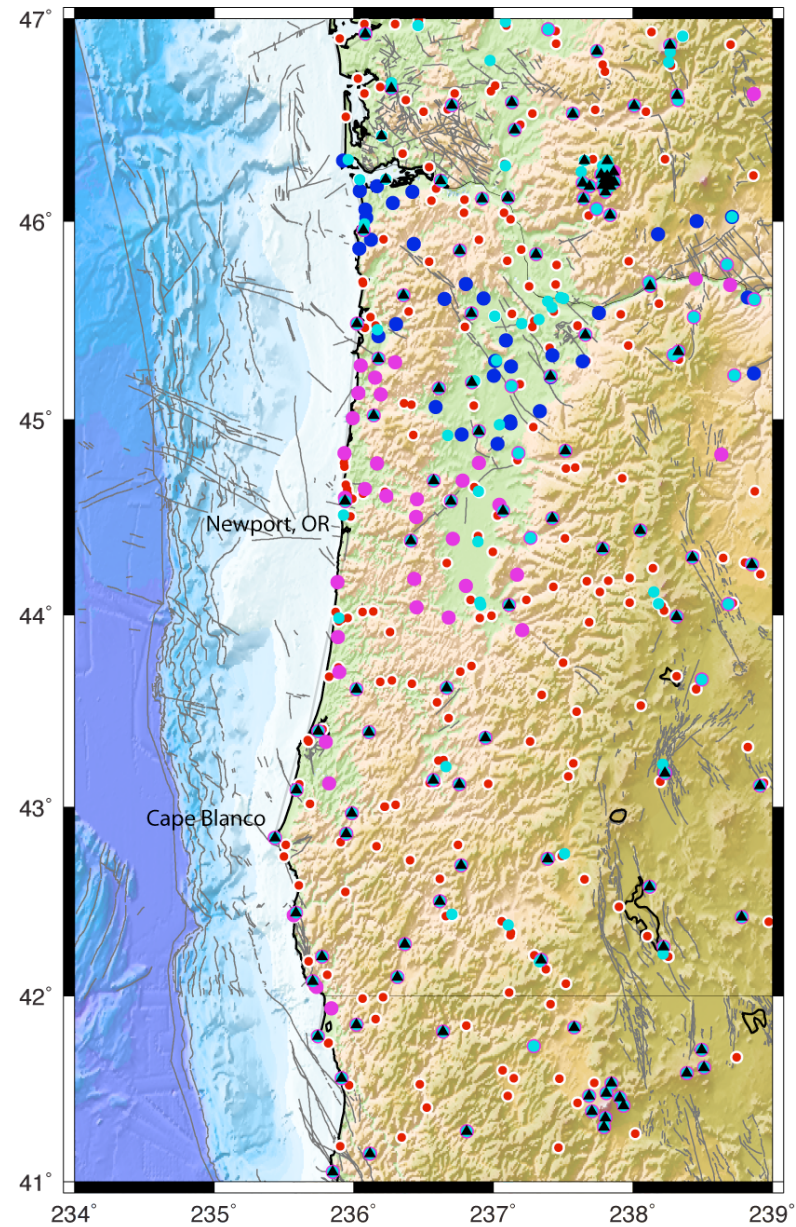


Figure 1. Map of coastal Oregon showing GPS site locations. Purple dots show locations of survey-mode GPS sites done by us in 2013 and 2014; blue were done by us in 2011 and 2012; turquoise dots are continuous GPS sites of the PANGA and PBO (with triangle) networks that we have included; and red dots are other survey-mode sites that we did not re-occupy recently.

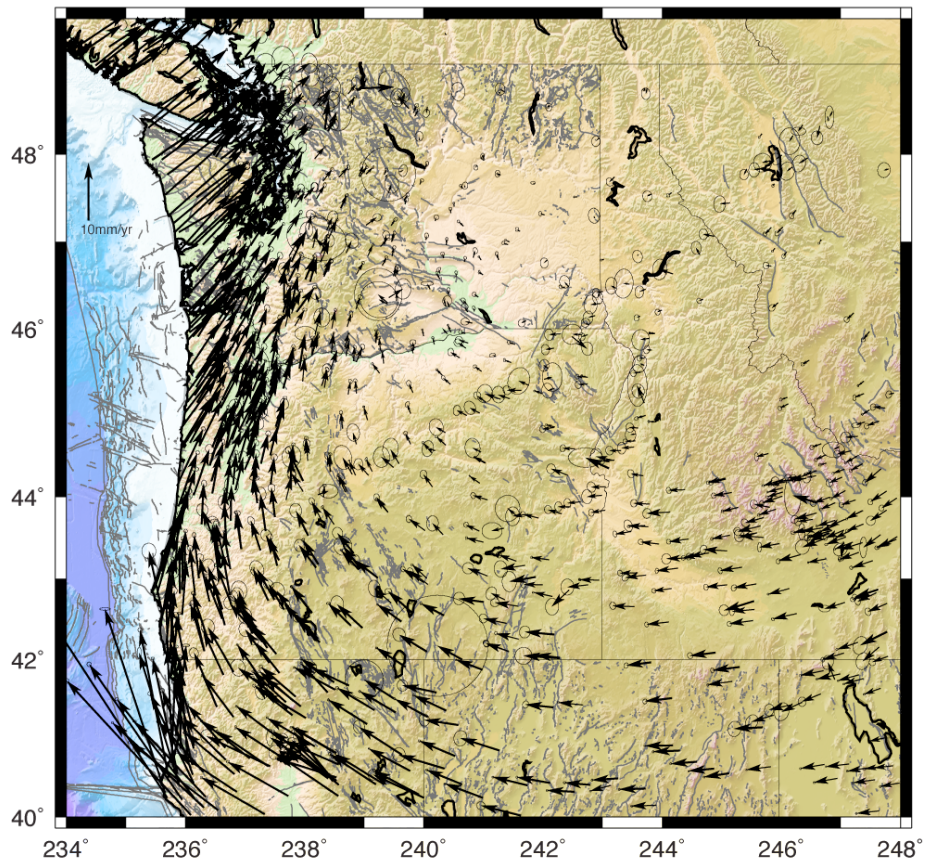


Figure 2. Pacific Northwest velocity field as of November 2014. Velocities are relative to North America with 70% confidence ellipses.

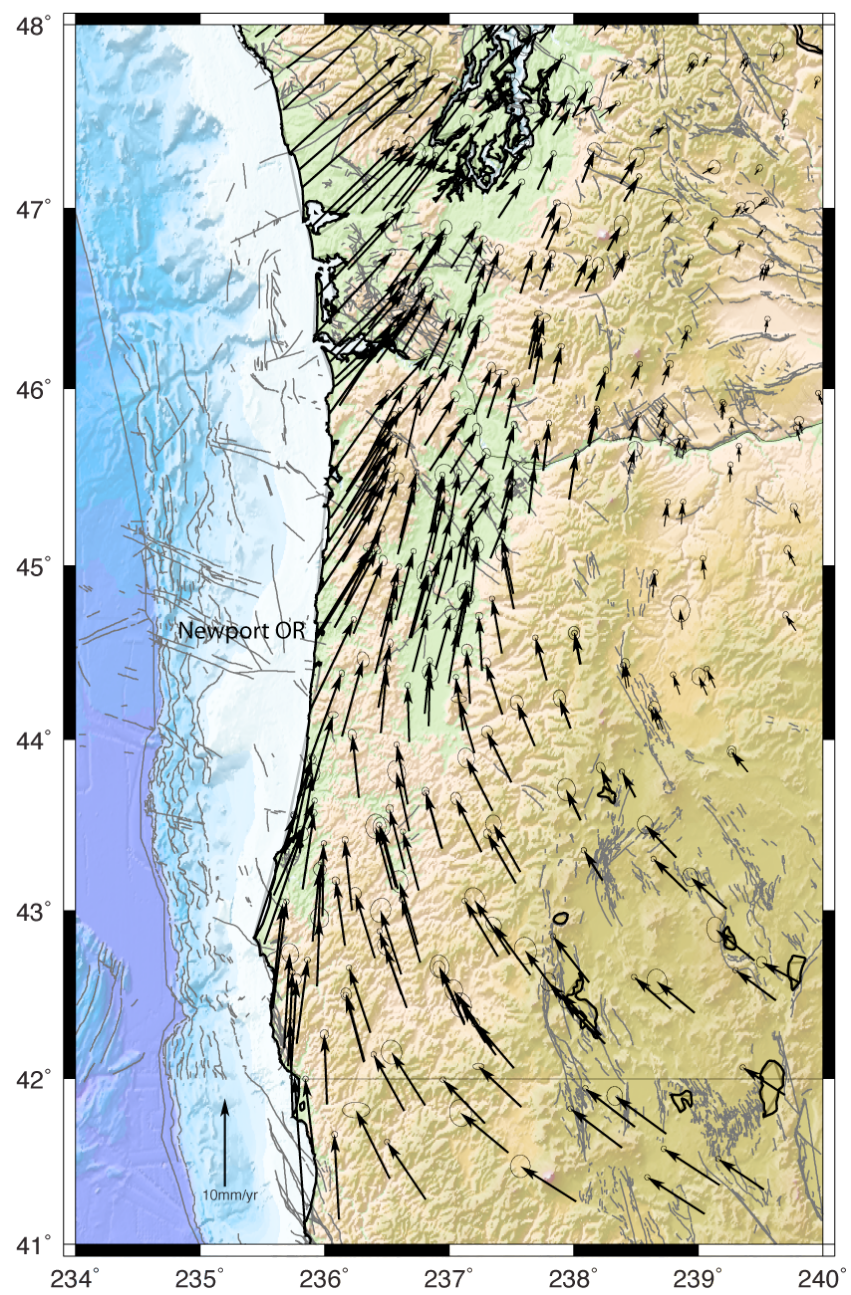


Figure 3. Coastal Oregon section of the Pacific Northwest velocity field as of November 2014.
Velocities are relative to North America with 70% confidence ellipses.

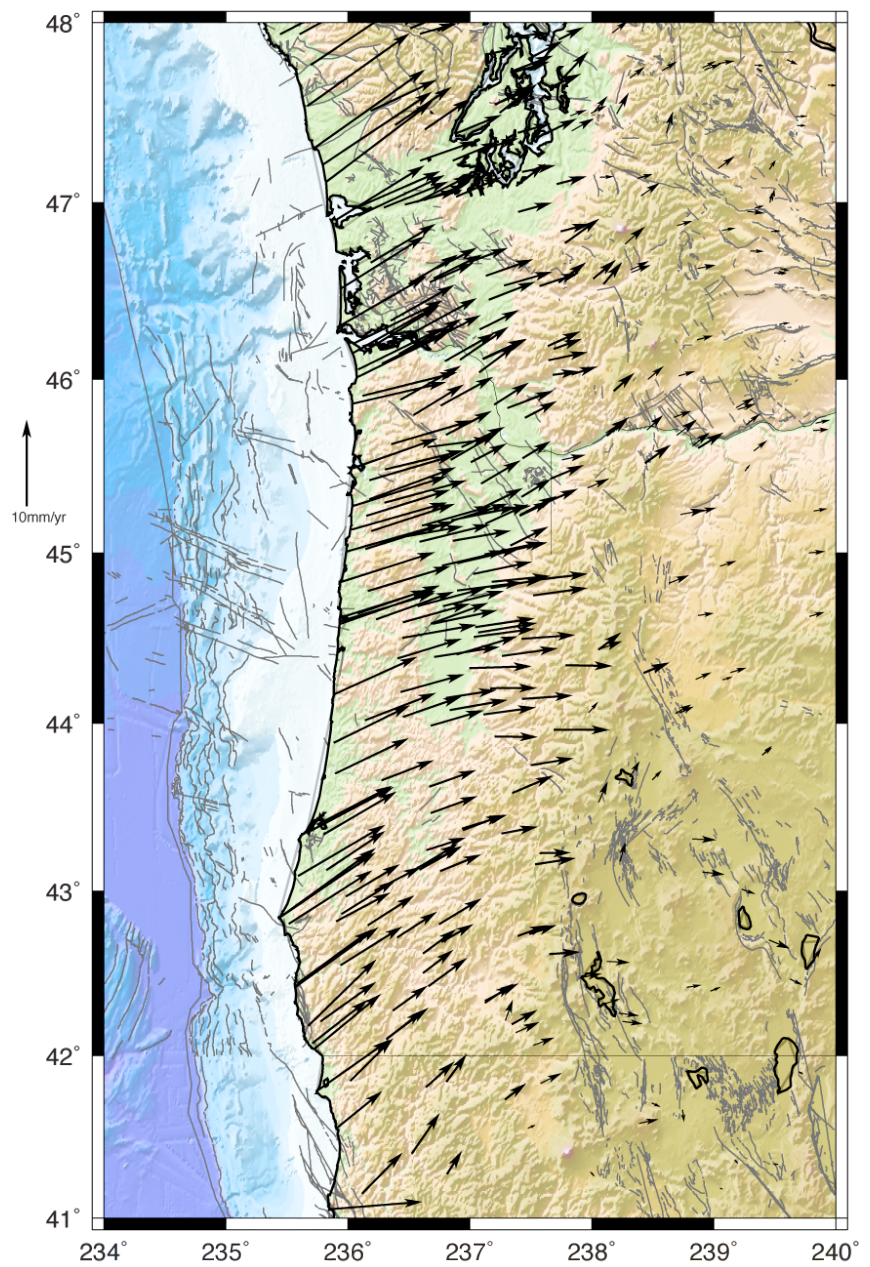


Figure 4. Coastal Oregon section of the Pacific Northwest velocity field as of November 2014. Velocities have had their rotations removed and are largely due to locking at the Cascadia subduction zone.

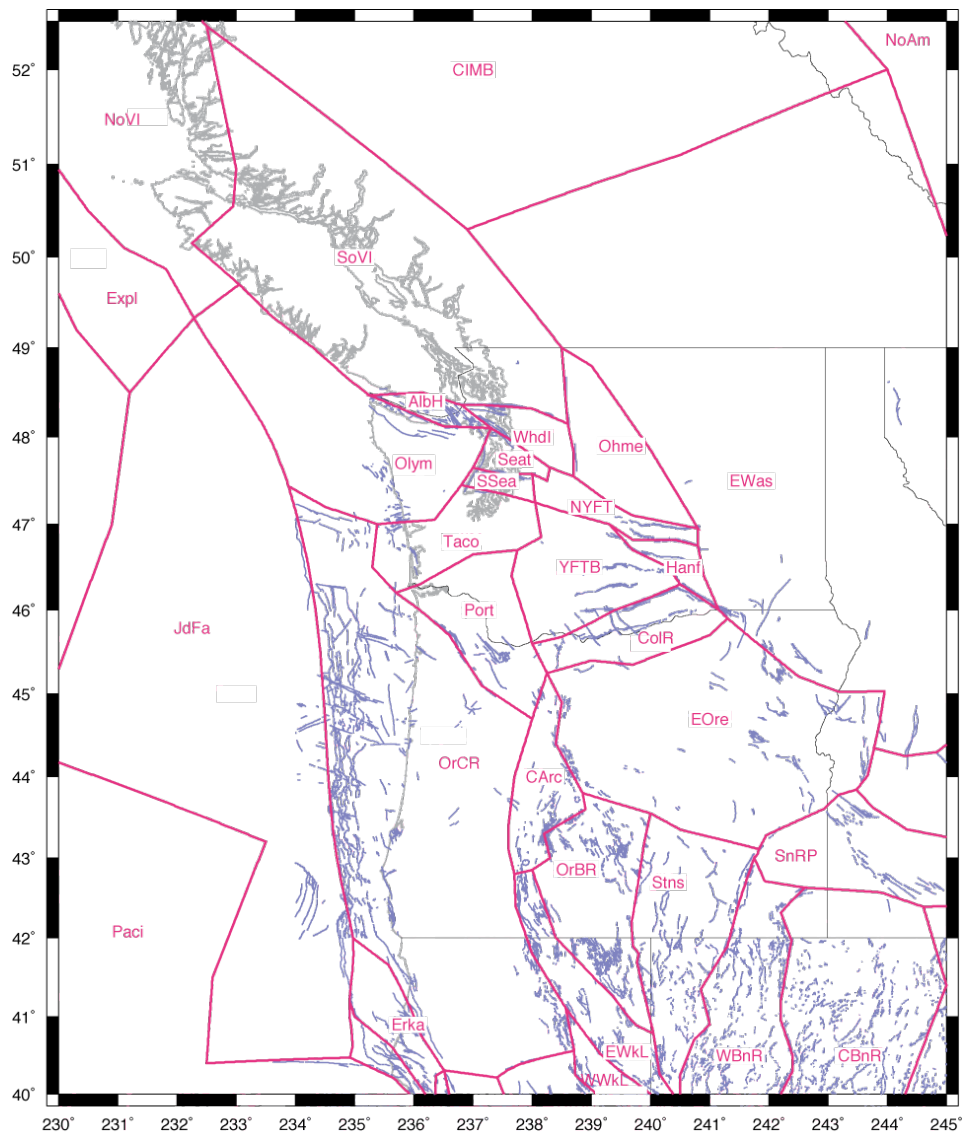


Figure 5. Block model of the Pacific Northwest used in estimation of locking at Cascadia. Motions of the blocks and strain rates across faults add to the complexity of the GPS velocity field and are accounted for with this model. Rotations of blocks and internal strain rates in some are estimated simultaneously with the Cascadia locking. Faults are from the USGS Q-fault database.

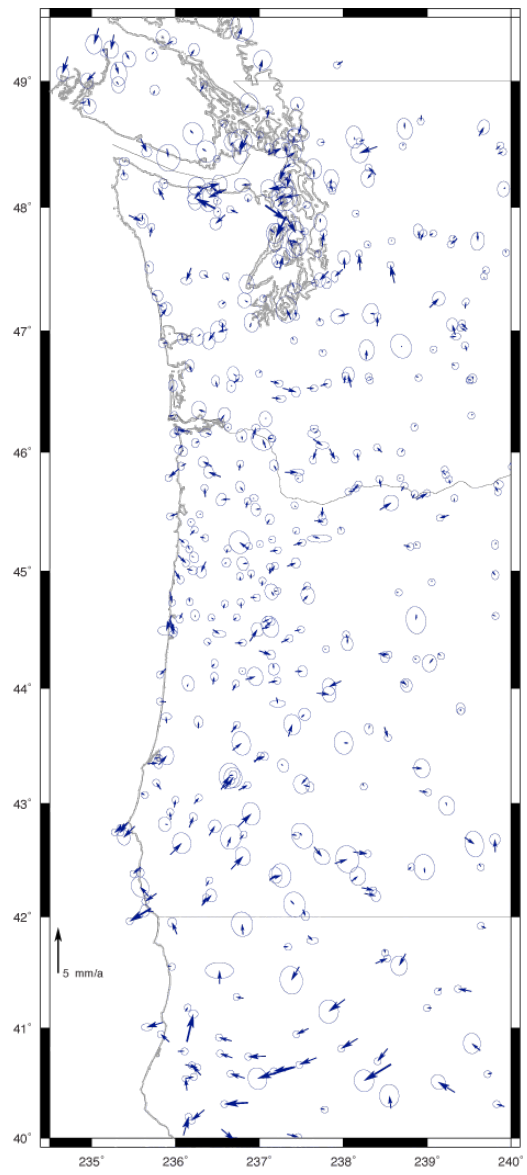
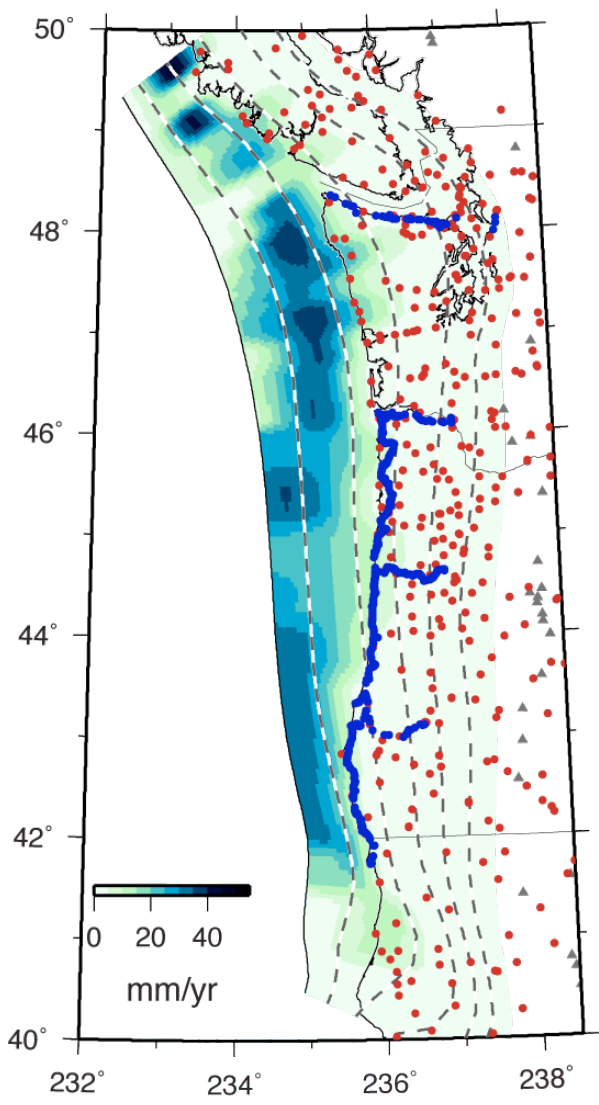


Figure 6. Model PN00. Locking is represented as a Gaussian function of depth. At left is the locking as a slip rate deficit. Red dots are locations of GPS sites and blue are leveling sites. Dashed contours of slab are at 10, 20, 30, 40 and 50 km depths. Triangles show locations of volcanoes. At right are the GPS residuals for this locking model with 70% confidence ellipses.

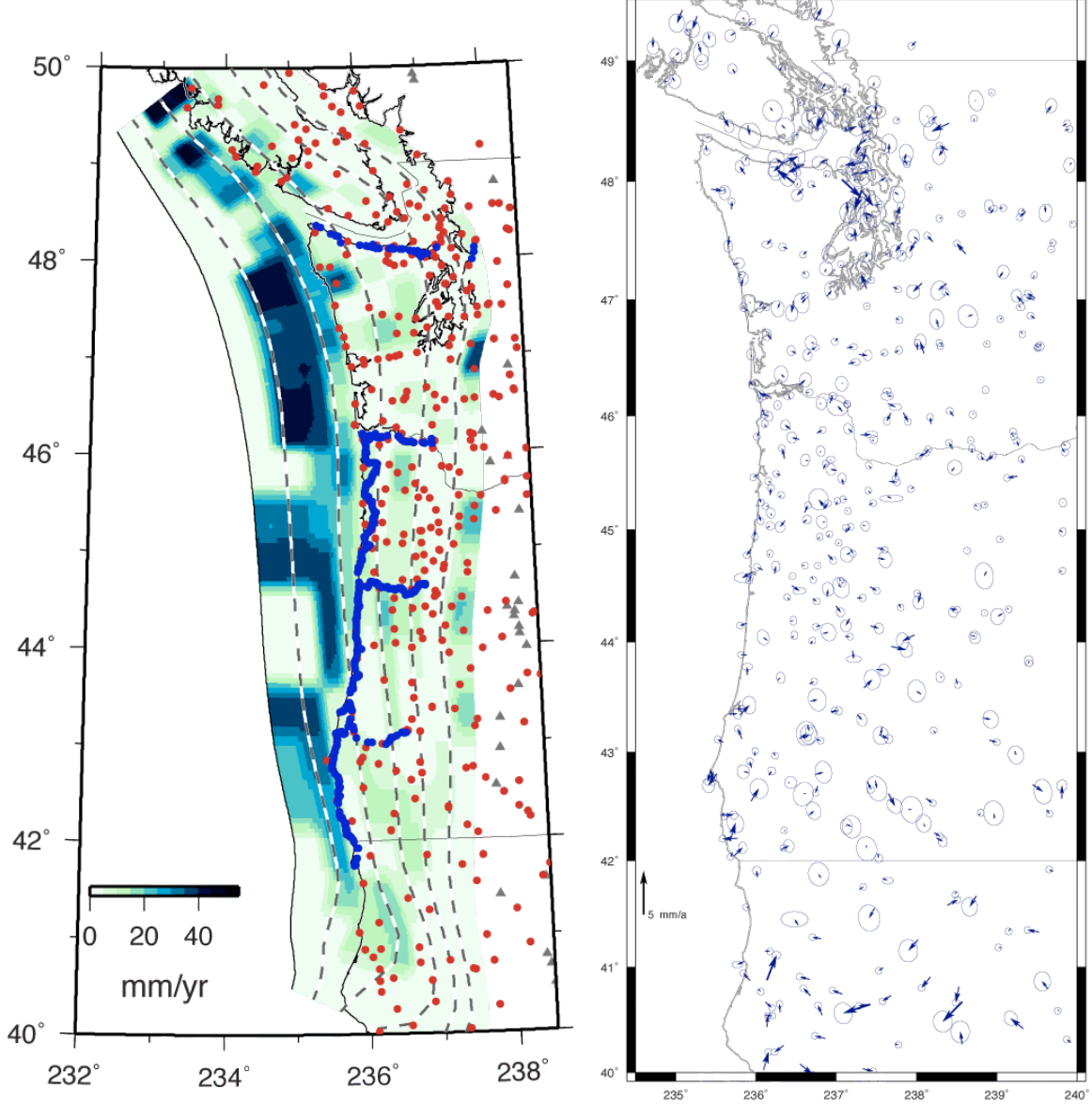


Figure 7. Model PN01. Locking is represented as a grid of nodes on the subduction fault. At left is the locking as a slip rate deficit. Red dots are locations of GPS sites and blue are leveling sites. Dashed contours of slab are at 10, 20, 30, 40 and 50 km depths. Triangles show locations of volcanoes. At right are the GPS residuals for this locking model.

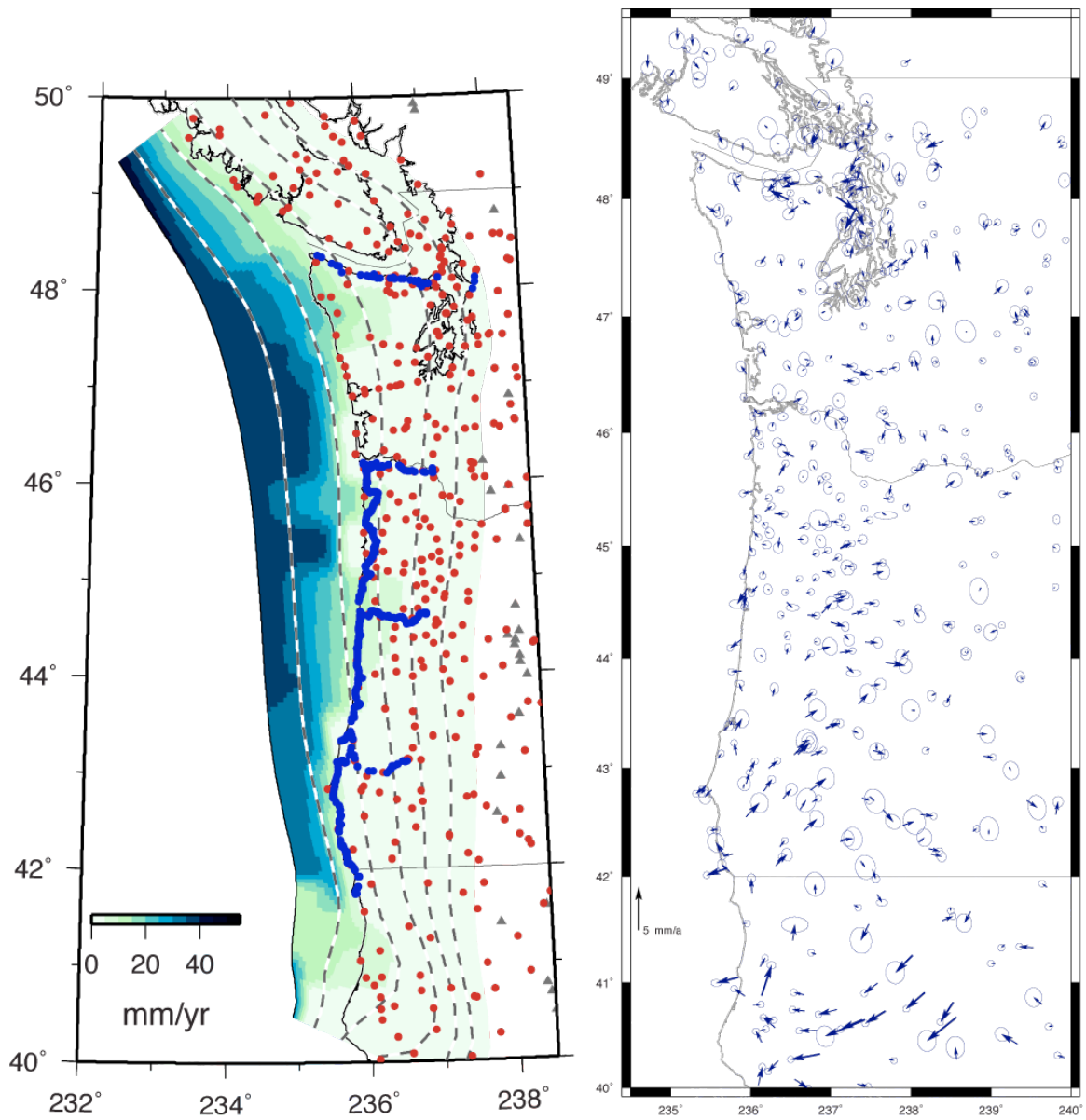


Figure 8. Model PN08. Locking is represented as an exponential function of depth and allowed to vary along strike. At left is the locking as a slip rate deficit. Red dots are locations of GPS sites and blue are leveling sites. Dashed contours of slab are at 10, 20, 30, 40 and 50 km depths. Triangles show locations of volcanoes. At right are the GPS residuals for this locking model.

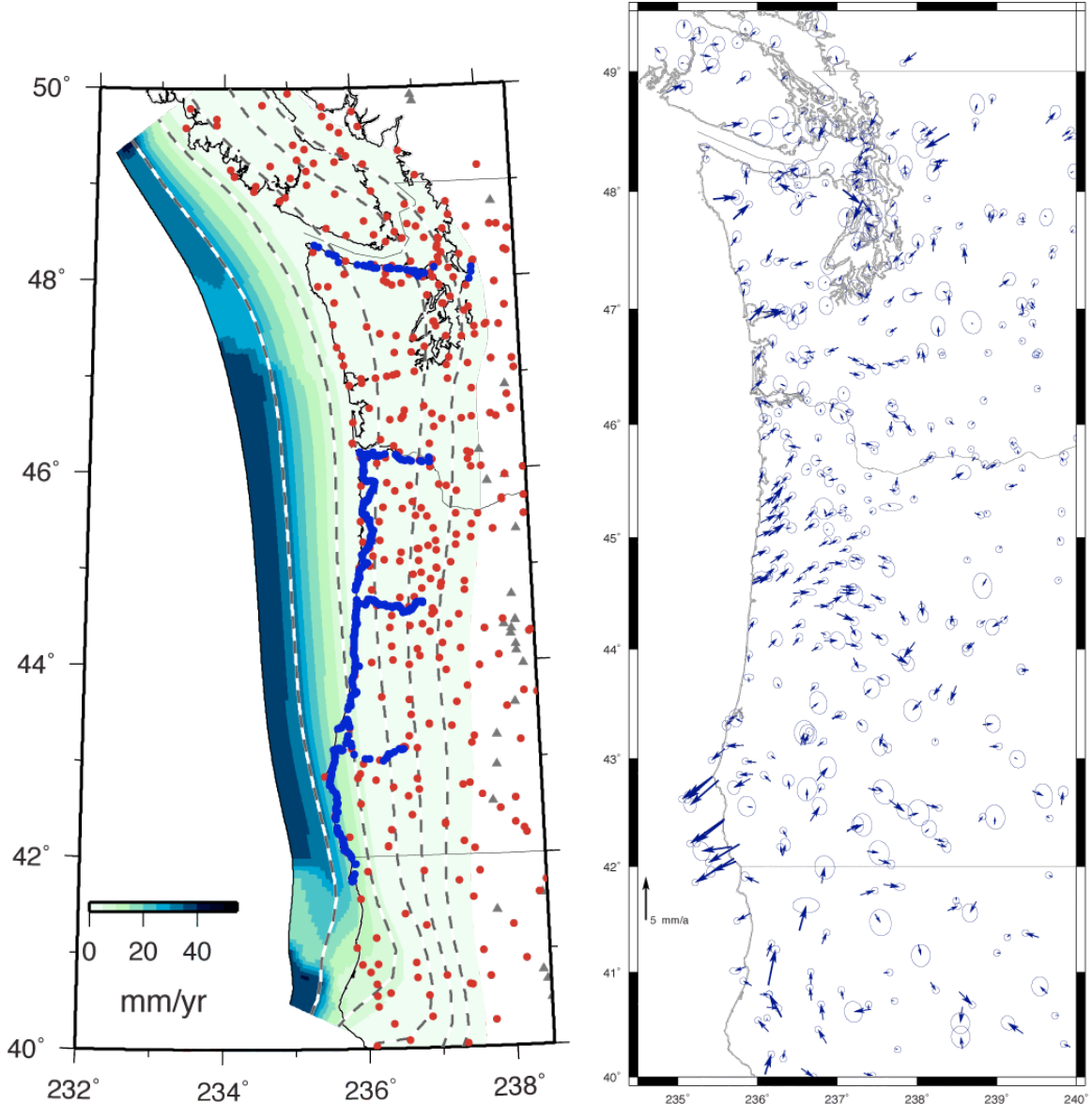


Figure 9. Model PN07. Locking is represented as an exponential function of depth and the locking fraction is assumed to not vary along strike (the slip rate deficit varies due to variation in the convergence vector along strike). At left is the locking as a slip rate deficit. Red dots are locations of GPS sites and blue are leveling sites. Dashed contours of slab are at 10, 20, 30, 40 and 50 km depths. Triangles show locations of volcanoes. At right are the GPS residuals for this locking model.

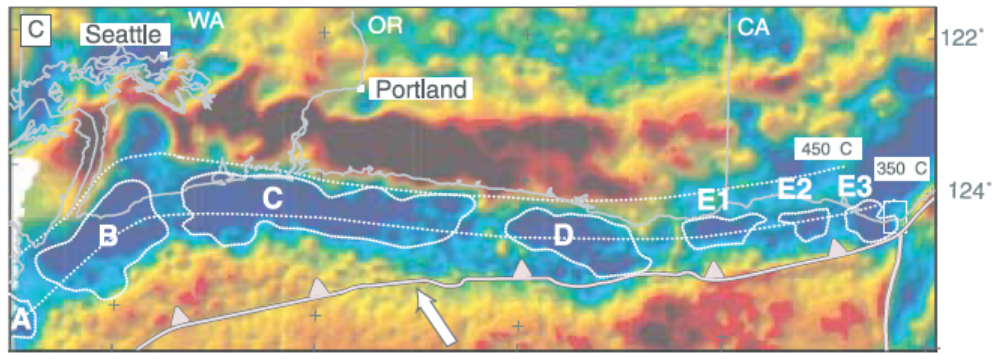


Figure 10a. Map of forearc basins along Cascadia from Wells et al. (2003). They propose that slip in great earthquakes may be concentrated below such basins. We test with GPS and leveling data (model PN11) whether or not modern loading of the subduction zone is similarly localized.

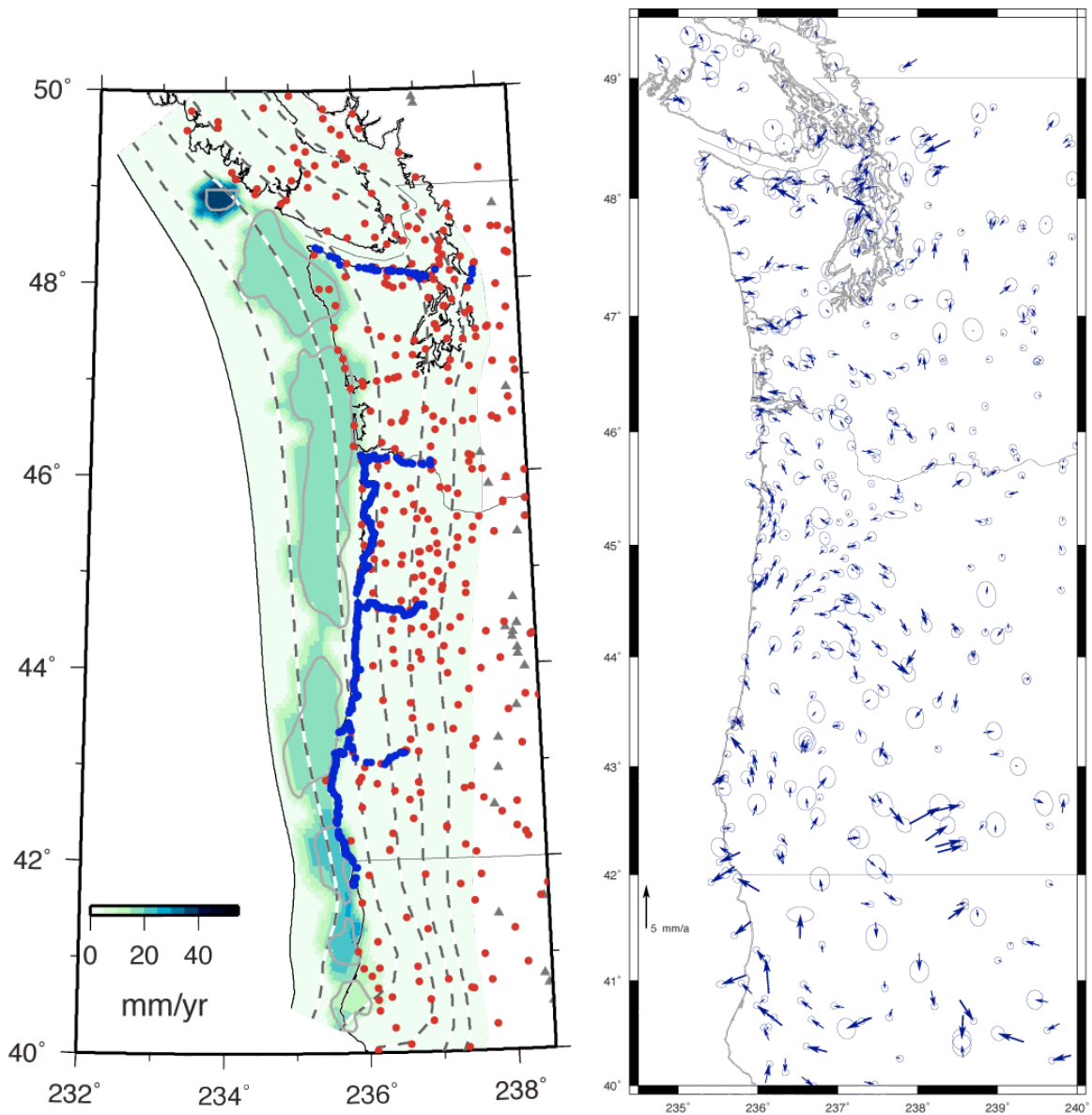


Figure 10b. Model PN11. Test of locking beneath forearc basins as suggested by Wells et al. (2003). Gray lines outline basins and color scale shows degree of locking. Red dots are locations of GPS sites and blue are leveling sites. Dashed contours of slab are at 10, 20, 30, 40 and 50 km depths. Triangles show locations of volcanoes. At right are the GPS residuals for this locking model with 70% confidence ellipses.

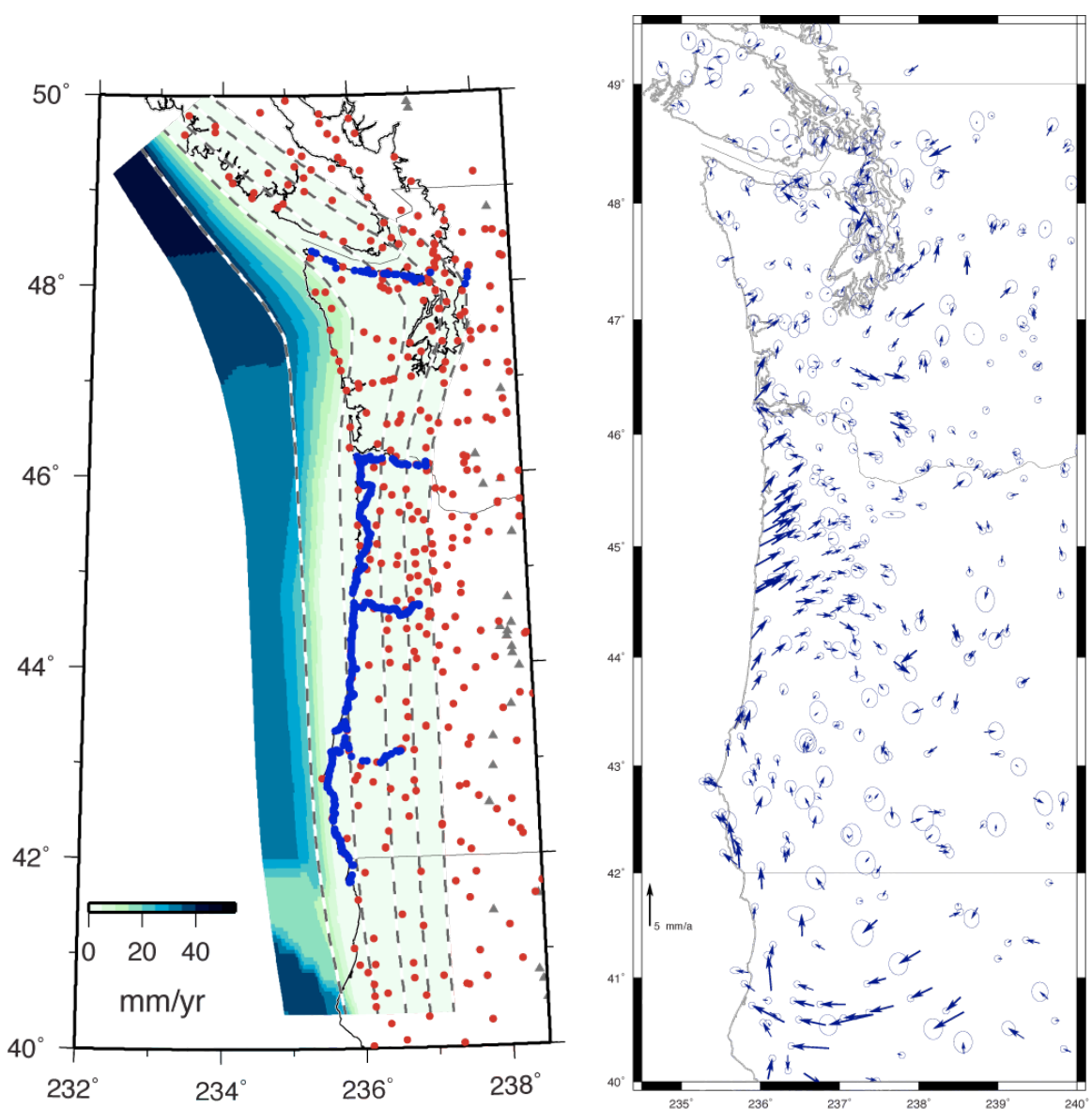


Figure 11. Model PN14. Test of locking as suggested by Fluck et al (1997). At left is the locking as a slip rate deficit. Red dots are locations of GPS sites and blue are leveling sites. Dashed contours of slab are at 10, 20, 30, 40 and 50 km depths. Triangles show locations of volcanoes. At right are the GPS residuals for this locking model with 70% confidence ellipses.

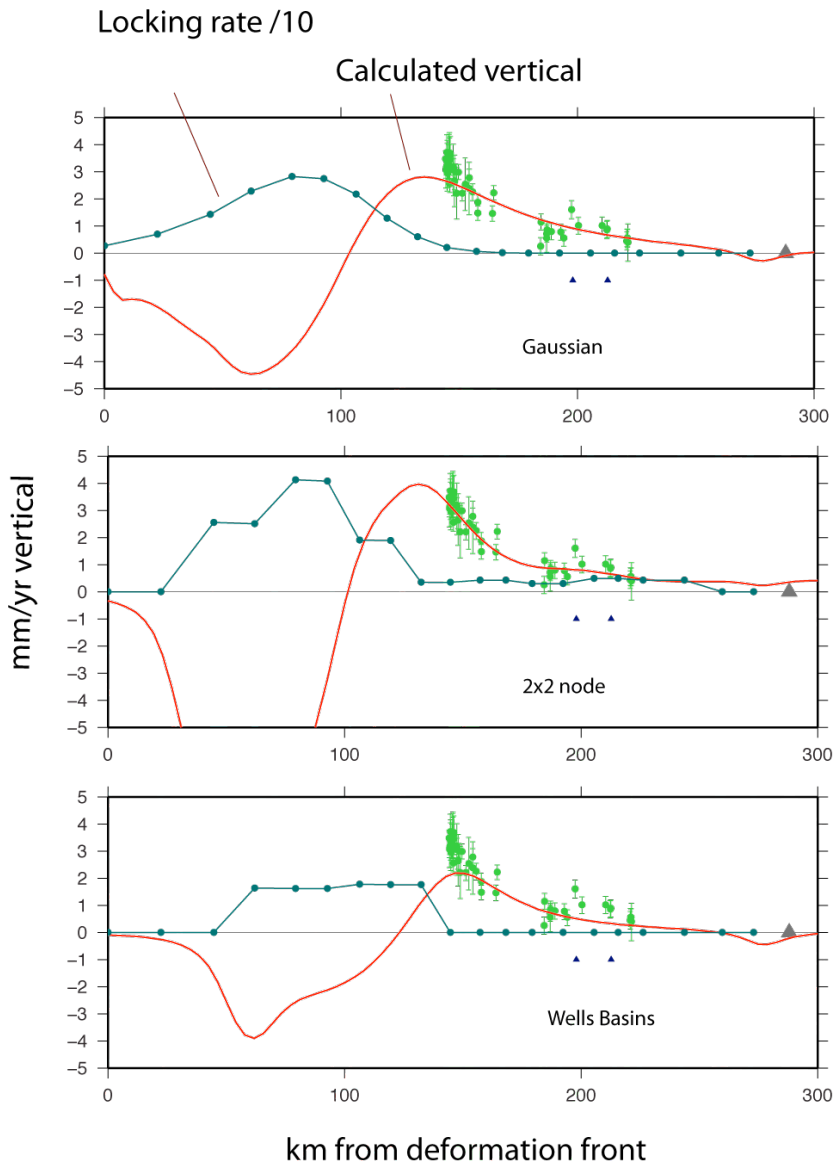


Figure 12. Profiles of vertical rates across the margin at 46.25N (Columbia River) for the models PN00 (top), PN01 (middle) and PN11 (bottom). Green symbols are observed uplift rates with one-sigma uncertainties, and red curves are predicted uplift rates. The green curve is the estimated locking rate in mm/yr reduced by a factor of 10.

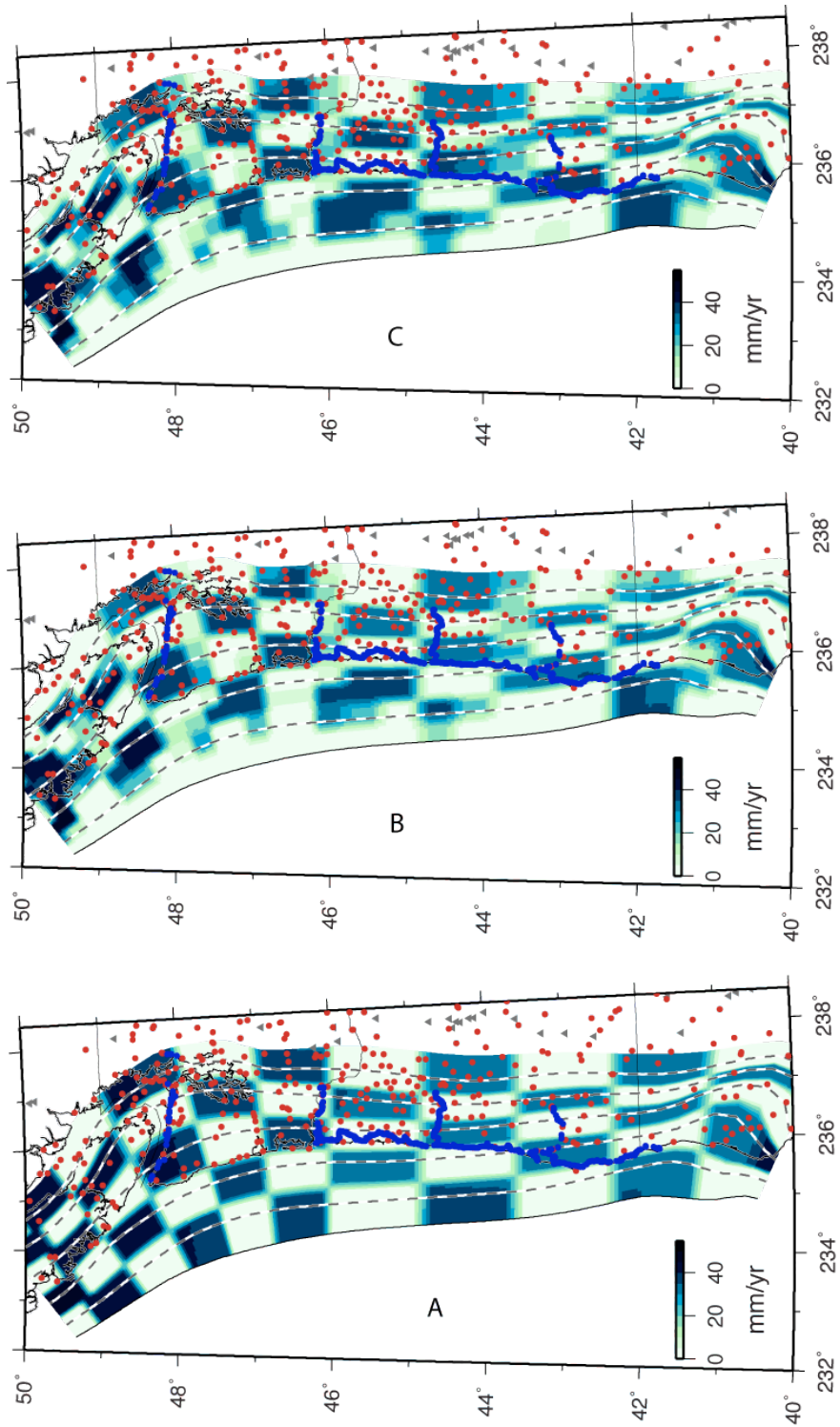


Figure 13. Checkerboard test of locking resolution. At bottom (A) is the test distribution of locking shown as a slip rate deficit. B and C are two models recovered from the inversion of data generated from A with random noise added. In B the starting model is a fully locked fault and in C it is a fully unlocked fault. Red dots are locations of GPS sites and blue are leveling sites. Dashed contours of slab are at 10, 20, 30, 40 and 50 km depths. Triangles show locations of volcanoes.